



## Abstract

The formation of secondary organic aerosol (SOA) generated by irradiating 2-methyl-3-buten-2-ol (MBO) in the presence and/or absence of  $\text{NO}_x$ ,  $\text{H}_2\text{O}_2$ , and/or  $\text{SO}_2$  was examined. Experiments were conducted in smog chambers operated either in dynamic or steady-state mode. A filter/denuder sampling system was used for simultaneously collecting gas and particle phase products. The structural characterization of gas and particulate products was investigated using BSTFA, BSTFA + PFBHA, and DNPH derivatization techniques followed by GC-MS and liquid chromatography analysis. This analysis showed the occurrence of more than 68 oxygenated organic compounds in the gas and particle phase, 28 of which were identified. The major components observed include 2,3-dihydroxyisopentanol (DHIP), 2-hydroxy-2-oxoisopentanol, 2,3-dihydroxy-3-methylbutanal, 2,3-dihydroxy-2-methylsuccinic acid, 2-hydroxy-2-methylpropanedioic acid, acetone, glyoxal, methylglyoxal, glycolaldehyde, and formaldehyde. Most of these oxygenated compounds were detected for the first time in this study.

While measurements of the gas phase photooxidation products have been made, the focus of this work has been an examination of the particle phase. SOA from some experiments was analyzed for the organic mass to organic carbon ratio (OM/OC), the effective enthalpy of vaporization ( $\Delta H_{\text{vap}}^{\text{eff}}$ ), and the aerosol yield. Additionally, aerosol size, volume, and number concentrations were measured by a Scanning Mobility Particle Sizer coupled to a Condensation Particle Counter system. The OM/OC was found to be 2.1 in MBO/ $\text{H}_2\text{O}_2$  system. The  $\Delta H_{\text{vap}}^{\text{eff}}$  was  $41 \text{ kJ mol}^{-1}$ , a value similar to that of isoprene SOA. The laboratory SOA yield measured in this study was found to be 0.7 % in MBO/ $\text{H}_2\text{O}_2$  for an aerosol mass of  $33 \mu\text{g m}^{-3}$ . Time profiles and proposed reaction schemes are provided for selected compounds.

The contribution of SOA products from MBO oxidation to ambient  $\text{PM}_{2.5}$  was investigated by analyzing a series of ambient  $\text{PM}_{2.5}$  samples collected in several places around the United States. In addition to the occurrence of several organic compounds in both field and laboratory samples, DHIP was found to originate only from

## SOA formation from the atmospheric oxidation of MBO

M. Jaoui et al.

Title Page

Abstract

Introduction

Conclusions

References

Tables

Figures

⏪

⏩

◀

▶

Back

Close

Full Screen / Esc

Printer-friendly Version

Interactive Discussion



the oxidation of MBO, and therefore this compound could serve as a tracer for MBO SOA. Initial attempts have been made to quantify the concentrations of DHIP and other compounds based on surrogate compound calibrations. The average concentrations of DHIP in ambient PM<sub>2.5</sub> samples from Duke Forest, NC ranged from zero during cold seasons in areas with low MBO emission rates to approximately 1 ng m<sup>-3</sup> during warm seasons in areas with high MBO emission rates. This appears to be the first time that DHIP has been detected in ambient PM<sub>2.5</sub> samples. The occurrence of several other compounds in both laboratory and field samples suggests that SOA originating from MBO can contribute under selected ambient conditions to the ambient aerosol mainly in areas where MBO emissions are high.

## 1 Introduction

Organic compounds of biogenic origin (BOCs) including isoprene, monoterpenes, sesquiterpenes, and oxygenated hydrocarbons are considered a significant class of organic species emitted from vegetation into the troposphere (Guenther et al., 1995). Since Went (1960) reported that oxidation of volatile organic compounds (VOC) emitted by plants could lead to the formation of organic aerosol, considerable efforts have been devoted in the last two decades to understand secondary organic aerosol (SOA) from ozonolysis reactions and ground-level ozone formation from BOCs (Kanakidou et al., 2005). SOA often constitutes a significant fraction of PM<sub>2.5</sub> and can have significant impact on the physical and chemical characteristics of ambient aerosol affecting air quality from global to regional and local scales. A number of studies have shown the roles of PM<sub>2.5</sub> in several atmospheric processes including visibility degradation (Sisler and Malm, 1994) and changes in radiative forcing that may affect the global climate (Charlson et al., 1992). Exposure to PM<sub>2.5</sub> has been implicated in increases in human mortality and morbidity levels and decreased PM levels have been shown to be associated with increased life expectancy (Pope et al., 2009). As the understanding of the toxicology associated with these particles develops, more accurate compositional data may be required.

## SOA formation from the atmospheric oxidation of MBO

M. Jaoui et al.

Title Page

Abstract

Introduction

Conclusions

References

Tables

Figures

◀

▶

◀

▶

Back

Close

Full Screen / Esc

Printer-friendly Version

Interactive Discussion



**SOA formation from  
the atmospheric  
oxidation of MBO**

M. Jaoui et al.

Title Page

Abstract

Introduction

Conclusions

References

Tables

Figures

◀

▶

◀

▶

Back

Close

Full Screen / Esc

Printer-friendly Version

Interactive Discussion



Oxygenated biogenic compounds are generally not considered significant contributors to SOA formation due to their low reactivity and low relatively emission rates compared to isoprene and monoterpenes (Guenther et al., 1995, 2006; König et al., 1995). One exception appears to be the compound, 2-methyl-3-butene-2-ol (MBO) which has been detected at high levels in ambient air and has been found to be produced and emitted in large quantities by many species of pine and fir trees (Goldan et al., 1993; Harley et al., 1998; Baker et al., 1999; Lamanna et al., 1999; Gray, 2008). Similar to isoprene, emissions of MBO have been found to be sensitive to light, temperature, and ecological factors (Harley et al., 1998; Gray, 2008). Moreover, its OH rate constant is similar to that of monoterpenes at  $5.8 \times 10^{-11} \text{ cm}^3 \text{ molec}^{-1} \text{ s}^{-1}$  (Carrasco et al., 2007). At present, the importance of MBO to atmospheric SOA formation is not well known, but its contribution could be significant in forested areas dominated by pine and fir trees. Recent studies have shown MBO levels as high as 6 ppb which in some cases has exceeded that from isoprene and monoterpenes (Spaulding et al., 2003; Goldan et al., 1993).

Detection of MBO specific reaction products in chamber and ambient field measurements suggests further evidence of its possible influence in regions with high MBO emissions (Spaulding and Charles, 2002). Although emissions of MBO have been estimated on a global basis to be 9.6 Tg per year the rapid oxidation of this compound leads to contributions to  $\text{HO}_x$  chemistry producing ozone, formaldehyde, acetone, and other carbonyl compounds (Steiner et al., 2007; Spaulding and Charles, 2002). In addition, dicarbonyls possibly formed through secondary reactions can lead to the increased production of SOA in an aqueous or non-aqueous aerosol phase (Carlton et al., 2007; Liggio et al., 2005; Volkamer et al., 2007; Kroll et al., 2005).

The gas-phase oxidation of MBO has been investigated in several recent laboratory studies in both the presence and absence of oxides of nitrogen ( $\text{NO}_x$ ). Most work to date has used smog chambers for studying the gas-phase kinetics of MBO oxidation, but in only a few cases have aerosol products been examined, as well. Fantechi et al. (1998) examined the gas-phase products from the reaction of MBO with

OH and NO<sub>3</sub> radicals, as well as ozone. The major carbonyl products from the initial reaction were glycolaldehyde and 2-hydroxy-2-methylpropanal. Additional organic products included acetone, formaldehyde, and formic acid from the OH and ozone reactions; acetone and organic nitrates were observed during the NO<sub>3</sub> reaction. Alvarado et al. (1999), Noda and Ljungstrom (2002), and Carrasco et al. (2007) studied the oxidation of MBO with O<sub>3</sub> and NO<sub>3</sub> and found similar results. Only a single study (Chan et al., 2009) has examined aerosol formation from the irradiated MBO system in the presence and absence of NO<sub>x</sub>. In that study, the photolysis of HONO served as a source of OH radicals in the presence of NO<sub>x</sub> and the photolysis of H<sub>2</sub>O<sub>2</sub> in the absence of NO<sub>x</sub>. They observed negligible SOA yields in the presence of NO<sub>x</sub> but measurable yields (0.10–0.14 %) in the absence of NO<sub>x</sub>. Only a limited number of organic reaction products were reported.

Given the uncertainties in both the emission and aerosol yields from the atmospheric oxidation of MBO, additional studies are needed to provide a more complete understanding of SOA formation from this compound. The present study examines both gas and aerosol products from MBO photooxidation. The gas phase products have been determined using both derivatization and non-derivatization techniques. Aerosol yields and other aerosol properties have been evaluated in the presence and absence of NO<sub>x</sub>. Moreover, a detailed examination of organic compounds comprising the aerosol has also been undertaken with the intent of identifying possible unique tracer compounds in ambient aerosol. Previously described tracer methods (Kleindienst et al., 2007) are then used to determine the extent to which such compounds can be used to estimating the contribution of organic aerosol in ambient air from MBO. The level of such tracer compound(s) are then evaluated from field samples. Finally, the effect of acidic sulfate aerosol is studied to determine the possible role of acidity on MBO SOA formation.

**SOA formation from  
the atmospheric  
oxidation of MBO**

M. Jaoui et al.

Title Page

Abstract

Introduction

Conclusions

References

Tables

Figures

⏪

⏩

◀

▶

Back

Close

Full Screen / Esc

Printer-friendly Version

Interactive Discussion



## 2 Experimental methods

### 2.1 Apparatus and reactants

The experiments were conducted in a 14.5 m<sup>3</sup> stainless-steel, fixed-volume chamber with walls having a 40 μm TFE Teflon coating. The chamber incorporate a combination of fluorescent bulbs to provide radiation distributed over the actinic portion of the spectrum similar to solar radiation, from 300–400 nm. For some irradiations without NO<sub>x</sub> present, UV-313 sunlamps were also used. The chamber was operated as a conventional batch reactor, or for experiments requiring a large sampling volumes, the chamber was operated in a flow mode to produce a steady-state concentration of gas and particle phase reaction products. The temperature and relative humidity within the chamber were determined with an Omega Engineering, Inc. (Stamford, CT) digital thermo-hygrometer (Model RH411). Light intensity was continuously monitored with an integrating radiometer (Eppley Laboratory, Inc., Newport, RI). Additional details of the chamber and its operation have been described by Kleindienst et al. (2006).

Experiments were conducted either in the presence or absence of NO<sub>x</sub>. For experiments with NO<sub>x</sub>, the photolysis of methyl nitrite (CH<sub>3</sub>ONO) was the primary initial source of hydroxyl radicals (OH) for some experiments. MBO, CH<sub>3</sub>ONO, and NO were added to the chamber through flow controllers to the target concentration. For experiments in the absence of NO<sub>x</sub>, the photolysis of hydrogen peroxide (H<sub>2</sub>O<sub>2</sub>) was the source of OH. H<sub>2</sub>O<sub>2</sub> as a 50 % aqueous solution was injected through a syringe pump into a heated glass bulb where it vaporized and then was mixed rapidly by the main dilution air flow. H<sub>2</sub>O<sub>2</sub> concentrations were determined by UV absorption using a conventional ozone monitor, as described previously (Kleindienst et al., 2009). For these experiments, MBO was added as described above. In some experiments, SO<sub>2</sub> was added to the chamber as a reactant to determine the effect of acidic sulfate aerosol in the formation of submicron organic aerosol products. Ammonium sulfate seed aerosol at ~1 μg m<sup>-3</sup> was also introduced into the chamber for all experiments to serve as a condensing medium for semivolatile organic products that might form.

## SOA formation from the atmospheric oxidation of MBO

M. Jaoui et al.

Title Page

Abstract

Introduction

Conclusions

References

Tables

Figures

◀

▶

◀

▶

Back

Close

Full Screen / Esc

Printer-friendly Version

Interactive Discussion



## 2.2 Gas phase measurements

NO and NO<sub>x</sub> were monitored with a TECO (Franklin, MA) oxides of nitrogen analyzer (Model 42C) with an in-line nylon filter used to prevent nitric acid from entering the analyzer. Ozone was measured with a Bendix (Lewisburg, WV) ozone monitor (Model 8002). SO<sub>2</sub> was determined by pulsed fluorescence detection (Model 43A, TECO, Hopington, MA). Relative MBO concentrations in the inlet and within the chamber were measured in a semi-continuous fashion by gas chromatography with flame ionization detection (GC-FID).

Detailed measurements of MBO and selected carbonyls were measured using a Hewlett-Packard (HP) (Palo Alto, CA) GC-FID (Model 5890) and a HP GC-MS (Model 6890 GC, w/Model 5972 MS). A fused (60 m × 0.32 mm inner diameter) column with a 1-μm DB-1 coating (J&W Scientific, Folsom, CA) was used for both GC systems. Liquid nitrogen was used to preconcentrate the analyte compounds in a sampling loop. The condensed organics were then injected onto the GC column using gas-sampling valves. The GC-FID and GC-MS operating parameters have previously been described by Blunden et al. (2005).

The identification and quantification of low molecular weight carbonyl and dicarbonyl compounds (e.g., formaldehyde, acetone, glyoxal, and methyl glyoxal) was achieved by derivatization with 2,4-dinitrophenyl-hydrazine (DNPH). In this technique, air samples were drawn through an impinger containing 5-ml of a DNPH/acetonitrile solution at a rate of 0.50 l min<sup>-1</sup>. Sampling times were typically 20 min. The samples were analyzed by HPLC/UV (Smith et al., 1989). The compounds formed during the reaction were identified and quantified from the chromatogram of a known set of sixteen hydrazones and dihydrazones run as an external standard. The technique also allows the concentrations of carbonyl compounds, for which standards are not available, to be estimated from the average molar extinction coefficient of the standard compounds. These hydrazones show a high degree of consistency, since the extinction coefficient is largely dependent only on the chromophore and not the substituent group (Smith et al., 1989).

### SOA formation from the atmospheric oxidation of MBO

M. Jaoui et al.

Title Page

Abstract

Introduction

Conclusions

References

Tables

Figures

⏪

⏩

◀

▶

Back

Close

Full Screen / Esc

Printer-friendly Version

Interactive Discussion



**SOA formation from  
the atmospheric  
oxidation of MBO**

M. Jaoui et al.

Title Page

Abstract

Introduction

Conclusions

References

Tables

Figures

◀

▶

◀

▶

Back

Close

Full Screen / Esc

Printer-friendly Version

Interactive Discussion



Higher molecular-weight carbonyl and hydroxylated compounds were collected with a 60-cm, 4-channel XAD4-coated annular denuder. The denuders were analyzed for organic compounds by extracting them in a 1:1 dichloromethane/methanol (DCM/MeOH) mixture and then derivatizing with O,N-pentafluorobenzyl hydroxylamine (PFBHA) followed by a second derivatization with bis(trimethylsilyl) trifluoroacetamide (Jaoui et al., 2004). Ketopinic acid (KPA) was used as internal standard. Extracts were then analyzed by GCMS using the techniques described below.

### 2.3 Aerosol phase measurements

Organic carbon concentrations were measured using a semi-continuous elemental carbon-organic carbon (EC-OC) instrument (Sunset Laboratories, Tigard, OR). The instrument operates with a quartz filter positioned within the oven housing used for the analysis. The pumping system drew chamber effluent through the filter at a rate of 8 l min<sup>-1</sup>. A carbon-strip denuder was placed in-line before the quartz filter to remove gas-phase organic compounds in the effluent which might interfere with the organic carbon measurement. With a sample collection time of 0.5 h and an analysis time of 0.25 h, the duty cycle for the measurement of OC was 0.75 h.

Aerosol size distribution, volume, and total number density were measured with a Scanning Mobility Particle Sizer (SMPS) (Model 3071A, TSI, Inc., Shoreview, MN) and a Condensation Particle Counter (CPC) (Model 3010, TSI, Inc., Shoreview, MN). The operating conditions for SMPS were as follows: sample flow – 0.2 l min<sup>-1</sup>; sheath flow – 2 l min<sup>-1</sup>; size scan from 19 to 982 nm. The SMPS was also used to determine effective enthalpies of vaporization of MBO aerosol by adding a heated inlet which allows the aerosol to be subjected to a range of temperatures (Offenberg et al., 2006).

The aerosol formed in the chamber was also collected with 47-mm glass-fiber filters (Pall Gelman Laboratory, Ann Arbor, MI) for off-line analysis. Samples were collected at a flow rate of 15 l min<sup>-1</sup>. These samples were then extracted by sonication with methanol. The filter extracts were then derivatized with BSTFA (Jaoui et al., 2004).

All extracts were analyzed by GC-MS on a ThermoQuest (Austin, TX) GC coupled with an ion trap mass spectrometer. The injector, heated to 270 °C, was operated in splitless mode. Compounds were separated on a 60-m, 0.25-mm-i.d., RTx-5MS column (Restek, Inc., Bellefonte, PA) having a 0.25- $\mu\text{m}$  film thickness. The oven temperature program started isothermally at 84 °C for 1 min followed by a temperature ramp of 8 °C  $\text{min}^{-1}$  to 200 °C, followed by a 2-min hold, then a second ramp of 10 °C  $\text{min}^{-1}$  to 300 °C. The ion source, ion trap, and interface temperatures were 200, 200, and 300 °C, respectively.

## 2.4 Laboratory procedures

For the batch-mode experiments (static mode) in the absence of  $\text{NO}_x$ , a known amount of liquid  $\text{H}_2\text{O}_2$  was injected into the chamber at the beginning of the experiment and allowed to stabilize for approximately 30 min. A known amount of liquid MBO was then added to the chamber. After a 5-min mixing period, the lights were turned on starting the reaction. Samples were then taken for gas and particle constituents at sampling times appropriate for the required masses needed for analysis. For experiments in the presence of  $\text{NO}_x$ , the reactants were added simultaneous to the chamber. In dynamic experiments, reactants were added to the chamber continuously and the effluent was withdrawn at the same flow rate for denuder and filter collection and on-line gas and particle analysis.

The chamber was operated as a batch reactor in experiments ER-462, ER-463 and ER-567, whereas in ER-464 and ER-465 the chamber was operated as a flow reactor with a nominal total flow of 60  $\text{l min}^{-1}$  to produce the steady-state reaction mixtures (Table 1). Some additional irradiations using MBO and  $\text{H}_2\text{O}_2$  were conducted in a second chamber, but these were conducted as survey experiments only and none of the data is reported here. The ER-464 experiment was conducted in two stages by irradiating MBO/ $\text{H}_2\text{O}_2$  mixtures in the absence (Stage 1) or presence (Stage 2) of  $\text{SO}_2$  to produce acidic sulfate aerosol. ER-465 experiment was also conducted in two stages by irradiating MBO/ $\text{CH}_3\text{ONO}/\text{NO}$  mixtures in the absence (ER-465a) or

## SOA formation from the atmospheric oxidation of MBO

M. Jaoui et al.

Title Page

Abstract

Introduction

Conclusions

References

Tables

Figures



Back

Close

Full Screen / Esc

Printer-friendly Version

Interactive Discussion



presence (ER-465b) of SO<sub>2</sub> to produce acidic sulfate aerosol. For these experiments, the reactant mixture at each stage was allowed to come to steady state over a period of 18–24 h before sampling began.

## 2.5 Field measurements

5 In addition to laboratory experiments, selected ambient PM<sub>2.5</sub> samples were collected on either quartz or Teflon-impregnated glass-fiber filters. Field sample filters were typically Soxhlet extracted. The resulting extracts were evaporated to dryness and derivatized with BSTFA (Jaoui et al., 2004). Detailed descriptions of some of these field campaigns have been provided by Lewandowski et al. (2007) and Kleindienst et al. (2010).  
10 The focus of the field sample analysis has been to determine the occurrence of MBO organic tracer compounds in ambient PM<sub>2.5</sub>.

## 3 Results and discussion

### 3.1 Initial conditions

15 The initial conditions for the experiments are given in Table 1. Initial MBO concentrations ranged from 15–19 ppm C. In the presence of NO<sub>x</sub>, CH<sub>3</sub>ONO (when used) and NO were each approximately 0.3 ppm; relative humidities were set to ~30%. For experiments in the absence of NO<sub>x</sub>, H<sub>2</sub>O<sub>2</sub> concentrations were 19 ppm in the static experiment and 7 ppm in the inlet for the dynamic experiment. Each dynamic run had a second stage where SO<sub>2</sub> was added to monitor the effect of acidic sulfate aerosol on the SOA yields and products; initial SO<sub>2</sub> was 0.21 ppm. As noted, ammonium sulfate at  
20 approximately 1 μg m<sup>-3</sup> was added to the reaction mixture to aid in secondary product condensation onto chamber aerosols.

A small amount of isoprene was detected by GC-FID at the beginning of some of the experiments, which is likely to be an artifact of MBO dehydration and result in isoprene

## SOA formation from the atmospheric oxidation of MBO

M. Jaoui et al.

Title Page

Abstract

Introduction

Conclusions

References

Tables

Figures

⏪

⏩

◀

▶

Back

Close

Full Screen / Esc

Printer-friendly Version

Interactive Discussion



formation during the injection, in the chamber, or during GC analysis (Tarvainen et al., 2005; Geron and Arnts, 2010). To evaluate the effect of temperature and humidity on MBO, a storage study was performed under dry and humid conditions using dual 30 l bags. Each bag was filled with 1  $\mu$ l of MBO and 25 l of zero hydrocarbon air. 40  $\mu$ l of pre-purified liquid water was added to one of the bags. Samples from each bag were analyzed by GC-FID and GC-MS during alternating 1-h periods. The results show that MBO conversion to isoprene occurred under dry conditions and up to 0.12 isoprene (mol mol<sup>-1</sup>) was observed under dry conditions compared to less than 0.02 under humid conditions, similar to that seen by Harley et al. (1998) and Lamanna et al. (1999). Moreover, the analysis showed that reduction of the temperature at several component locations of the pre-concentration system reduces MBO dehydration significantly. Thus, we estimate at most (and probably much less than) 1 % of MBO might have been converted to isoprene at the beginning of the dry experiments.

## 3.2 Gas-phase products

The analysis of laboratory generated gas phase and SOA products from MBO oxidation showed a series of organic compounds containing ketone, acidic, and/or alcoholic functional groups. Many of these compounds do not have authentic standards and some of the identifications were based on the interpretation of the mass spectra of the derivatized compounds. Thus, for compounds without authentic standards, identifications should be regarded as tentative. Detailed procedures for these approaches have been described in previous work (Jaoui et al., 2004, 2005).

### 3.2.1 Time profile of products

Figure 1a shows a standard photochemical time series of the major constituent in the batch reaction of MBO in the presence of NO<sub>x</sub>. Concentrations of MBO, O<sub>3</sub>, NO, and NO<sub>x</sub>-NO are shown for experiment ER-463. In the absence of a direct OH photolysis source such as CH<sub>3</sub>ONO, the consumption of MBO commences with only a small

## SOA formation from the atmospheric oxidation of MBO

M. Jaoui et al.

Title Page

Abstract

Introduction

Conclusions

References

Tables

Figures

◀

▶

◀

▶

Back

Close

Full Screen / Esc

Printer-friendly Version

Interactive Discussion



induction time given its very large OH rate constant of  $5.8 \times 10^{-11} \text{ cm}^3 \text{ molec}^{-1} \text{ s}^{-1}$  (Carrasro et al., 2007). The profiles of the inorganic species show the characteristics of a standard VOC/NO<sub>x</sub> irradiation.

For experiments in a batch mode, values for the SOA concentrations can also be determined from the SMPS measurements. These measurements have the advantage of having low limits of detections with reasonably good precision. SOA formation is difficult to distinguish at the beginning of the experiment involving only NO due to the presence of seed aerosol. However, once the initial NO is removed from the system due to reaction, SOA concentrations are seen to increase very slightly above the seed aerosol concentration as the ozone builds up in the chamber. This formation; although not quantifiable as a yield; is similar to that observed for monoterpene photooxidation in the presence of NO<sub>x</sub>.

Of greater interest are the carbonyl compounds formed during the irradiation shown in Fig. 1b. It is clear that the carbonyl products from the OH + MBO reaction are detected from the first DNPH sample taken at (0.7 h) with NO is still present in the system at relatively high concentrations. According to conventional reaction kinetics, OH adds to the double bond in MBO to form an RO<sub>2</sub> radical which oxidizes NO to NO<sub>2</sub> with the resultant alkoxy radical producing a carbonyl product. If OH adds to the least substituted position of MBO, glycolaldehyde and acetone result as the major carbonyl products. If OH is added to the most substituted position, scission of the alkoxy radical produces formaldehyde and 2-hydroxy-2-methylpropanal (2-HMP) as the predominant carbonyl products.

The elution order of the products was established from the external hydrazone standards mentioned previously. Formaldehyde and acetone formed in the reaction are clearly identified from their retention times. Hydroxycarbonyls have previously been reported (Grosjean and Grosjean, 1995) to have retention times that precede carbonyl compounds of the same carbon number. Thus, glycolaldehyde is detected between the hydrazones of formaldehyde and acetaldehyde and, in fact, is found to nearly co-elute with formaldehyde. Since standards are available, the formation of 2-HMP was

**SOA formation from  
the atmospheric  
oxidation of MBO**

M. Jaoui et al.

Title Page

Abstract

Introduction

Conclusions

References

Tables

Figures

◀

▶

◀

▶

Back

Close

Full Screen / Esc

Printer-friendly Version

Interactive Discussion



rationalized based on a retention time and elution order of the DNPH derivative between the formaldehyde and acetaldehyde derivatives (Grosjean and Grosjean, 1995). Under the conditions of these experiments, except for acetone, these compounds all have very rapid OH rate constants ( $> 1 \times 10^{-11} \text{ cm}^3 \text{ molec}^{-1} \text{ s}^{-1}$ ) and thus yields for the carbonyls are very difficult to determine in the absence of secondary OH reaction and photolysis.

Secondary reactions of glycolaldehyde and acetone are known to produce the dicarbonyl compounds, glyoxal and methyl glyoxal, respectively. Glyoxal (GLY) was detected at relatively high levels during the irradiation, as seen in Fig. 1b, whereas methyl glyoxal (MGLY) was formed at low levels. This finding reflects the factor of 50 differences in OH rate constants for glycolaldehyde and acetone. While photolysis rate constants are less well established, it is possible that photolysis contributed to some degree to the formation of methyl glyoxal by acetone. Finally while glyoxal was identified by retention time with authentic standards, there is the possibility that the derivative for glyoxal might have formed from a partially acidic alcoholic hydrogen from glycolaldehyde. However, previous measurements suggest that the process is too slow to be of much importance (Smith et al., 1989). Nonetheless, this possibility cannot be completely excluded although efforts were made to render this process negligible. Two peaks (unkn 1 and unkn 2: Fig. 1b) were detected with a relatively high concentrations, these compounds could not be identified in this study. The importance of the dicarbonyl compounds rest in their possible significance for the formation of organic aerosol.

### 3.2.2 Characterization of gas-phase products from denuder sampling

A qualitative analysis was performed of the gas-phase products for experiments involving the presence or absence of  $\text{NO}_x$ . The analysis uses the PFBHA + BSTFA double derivatization of a denuder extract. While this technique is an integrated technique that requires long sampling times, it does provide a sensitive method for measuring low concentrations of highly oxidized organic compounds, possibly semivolatile compounds in the gas phase. Thus, products found by this collection technique could be informative

## SOA formation from the atmospheric oxidation of MBO

M. Jaoui et al.

Title Page

Abstract

Introduction

Conclusions

References

Tables

Figures



Back

Close

Full Screen / Esc

Printer-friendly Version

Interactive Discussion



for possible precursors for the types of compounds that may form in the particle phase. However, for light organics, even those that are polar, the XAD-4 coated denuder acts as a chromatograph and low molecular weight carbonyl compounds tend to elute from the denuder during the course of an extended collection.

5 Figure 2 shows a GC-MS chromatogram from a MBO photooxidation in the absence of  $\text{NO}_x$  (ER-462). Several major peaks were detected in the gas phase including 2,3-butanedione; 2,3-dioxobutanal; 2-oxopropane-1,3-dial; 2-hydroxypropane-1,3-dial; 2,3-dioxobutane-1,4-dial; 2,3-dihydroxy-2-methylbutanedialdehyde, glyoxal, and methylglyoxal. While formaldehyde, acetone, glycolaldehyde, and 2-HMP have been  
10 previously reported (see above; also Fantechi et al., 1998; Alvarado et al., 1999; Chan et al., 2009), the aldehydic compound are highly reactive and are not detected at high concentrations by this technique at this stage of the reaction. That stated, 2-HMP was identified based on an interpretation of the mass spectrum of a peak at a retention time of 25.5 min, although at very low abundances. Its mass spectrum shows frag-  
15 ments ( $M^{+} +1$ ,  $M^{+} -15$ ,  $M^{+} -89$ ) similar to those fragments reported in the literature by Spaulding and Charles (2002). 2-HMP has been reported in chamber and ambient atmospheres at a low ppb mixing ratio (Spaulding et al., 2003; Spaulding and Charles, 2002; Kim et al., 2010) and has been used as evidence of the contribution of MBO oxidation in mainly forested atmospheres. In our study, chamber 2-HMP by the double  
20 derivative was detected at low levels, due in large part to the extensive degree of oxidation mainly through OH reaction and/or by photolysis. The reaction of 2-HMP leads to the formation of formaldehyde, acetone, and possibly methylglyoxal (e.g., Fantechi et al., 1998; Spaulding et al., 2003). In addition to these compounds, several highly oxidized hydroxyl/oxo/aldehydes were identified in this study and presented at the end  
25 of Table 2.

**SOA formation from  
the atmospheric  
oxidation of MBO**

M. Jaoui et al.

Title Page

Abstract

Introduction

Conclusions

References

Tables

Figures

◀

▶

◀

▶

Back

Close

Full Screen / Esc

Printer-friendly Version

Interactive Discussion



### 3.3 Particle-phase products

#### 3.3.1 Aerosol parameters

The production of aerosol was found to be highly dependent on the exact conditions under which the experiments were carried out, in particular the presence of  $\text{NO}_x$  in the system. This system produced only very low levels of aerosol, which was typically insufficient (using standard procedures for aerosol quantification) for determining aerosol parameters and detailed organic analysis. Except for a minor organic nitrate channel, the photooxidation system in the presence of  $\text{NO}_x$  converts virtually all  $\text{RO}_2$  formed into RO radicals, which then decompose or isomerizes to produce carbonyl or hydroxycarbonyl compounds (Atkinson, 2000). Without  $\text{NO}_x$  in the system,  $\text{RO}_2$  radical typically react with  $\text{HO}_2$  or self react to produce a product molecule with five carbons while adding functional groups to the product. These products are sufficiently nonvolatile to condense into the particle phase and the system without  $\text{NO}_x$  was the only one where aerosol parameters and composition were measured.

The secondary organic aerosol yield ( $Y_{\text{SOA}}$ ) and secondary organic carbon ( $Y_{\text{SOC}}$ ) are generally defined using the following relationships  $Y_{\text{SOA}} = \text{SOA}/\Delta\text{HC}$  and  $Y_{\text{SOC}} = \text{SOC}/\Delta\text{HC}_C$ , where SOC is the corrected organic carbon concentration,  $\Delta\text{HC}$  is the reacted hydrocarbon mass concentration, and  $\Delta\text{HC}_C$  is the reacted carbon mass concentration of the hydrocarbon obtained from Table 3. SOA was obtained from gravimetric measurement of the filter when there is a reasonable degree of consistency with the particle mass obtained from the SMPS volume assuming a density of unity. Organic carbon and organic aerosol yields were determined for some experiments where the chamber was operated in a dynamic mode. Uncertainties in the yields come from the experimental uncertainties in SOA and the reacted MBO concentrations.

Yields for some experiments conducted in this study are found in Table 3. The gravimetric yield values originated from the static experiments were considerably higher than those measured using the SMPS system. The SOA gravimetric mass was found to be overestimated during these static experiments because of the extended sampling

## SOA formation from the atmospheric oxidation of MBO

M. Jaoui et al.

Title Page

Abstract

Introduction

Conclusions

References

Tables

Figures

◀

▶

◀

▶

Back

Close

Full Screen / Esc

Printer-friendly Version

Interactive Discussion



**SOA formation from  
the atmospheric  
oxidation of MBO**

M. Jaoui et al.

[Title Page](#)[Abstract](#)[Introduction](#)[Conclusions](#)[References](#)[Tables](#)[Figures](#)[◀](#)[▶](#)[◀](#)[▶](#)[Back](#)[Close](#)[Full Screen / Esc](#)[Printer-friendly Version](#)[Interactive Discussion](#)

time and low SOA mass in the chamber at the end of the sampling period (due to dilution). For example, ER-463 was conducted in the presence of  $\text{NO}_x$ , and while a measurable SOA yield (0.2 %) was obtained from the gravimetric analysis, this value was considerably higher than that measured using the SMPS values. However, some experiments conducted in the presence of  $\text{H}_2\text{O}_2$  with and without acidic sulfate aerosol (ER-464a,b and ER-465b), organic aerosol was formed and measured using the carbon analyzer with carbon yields ( $Y_{\text{SOC}}$ ) ranging from 0.2 % to 0.9 %. The SOA yield was also found to be 0.7 % for the system in the absence of  $\text{NO}_x$  (ER464a). For all experiments with MBO, the yield tended to be systematically higher for experiments conducted under acidic conditions, particularly under high  $\text{NO}_x$  conditions. The implications of these findings are discussed below.

### 3.3.2 Characterization of SOA products

Sufficient aerosol masses collected on GF filters from the experiments were analyzed by GC-MS. The total ion chromatogram is shown in Fig. 3 for cases without (top) and with (bottom)  $\text{SO}_2$  respectively, for an irradiation of MBO using the photolysis of  $\text{H}_2\text{O}_2$  as the source of OH radicals. Mass spectra from the TIC shows the presence of more than 60 derivatized compounds (not all shown) in the absence of  $\text{NO}_x$ . In some cases, presumably semivolatile compounds have been detected both in the gas and particle phases. The approach for identifying individual product compounds is given as follows: All chromatograms are blank correct for peaks found in blank or background extracts. An identification number was then associated with each remaining peak only if its corresponding mass spectrum was consistent with the fragmentation pattern of a derivatized analyte (Jaoui et al., 2005) and any underivatized compounds are not considered. All recorded spectra were compared with spectra derived from reference compounds obtained from various sources including authentic standards, previous reports of a compound that have the same nominal mass spectrum, detection in the field samples, and finally an interpretation of the mass spectrum solely. Such a procedure was employed by Edney et al. (2003).

**SOA formation from  
the atmospheric  
oxidation of MBO**

M. Jaoui et al.

Title Page

Abstract

Introduction

Conclusions

References

Tables

Figures

◀

▶

◀

▶

Back

Close

Full Screen / Esc

Printer-friendly Version

Interactive Discussion



The GC-MS analysis shows the presence of several significant peaks (e.g., 8, 14, 20, 26, 36, 38, 39, 42, 46) in the particle phase. In addition, a large number of other smaller peaks were observed in the gas and particle phases, reflecting the complexity of the oxidation of MBO. Additional compounds (e.g., high molecular weight organics, organonitrates, organosulfates) could have been present in the SOA or the gas phase but could not be detected based on the analytical techniques used in this study. To facilitate discussion, compounds identified in the present study are listed in Table 2 along with their retention time, molecular weights of the derivatized compounds (when possible), and their mass fragments/adducts ( $m/z$ ) of the derivatives. A tentative identification for some compounds was also included in Table 2.

SOA generated from MBO oxidation is dominated by oxygenated compounds in which MBO double bonds are oxidized. The GC-MS analysis TIC chromatographic data for SOA from the oxidation of MBO in the presence of  $\text{H}_2\text{O}_2$  and  $\text{SO}_2$  shows the presence of eight significant peaks (8, 14, 16, 20, 22, 39, 42, and 46) in the SOA (ER-464b). By far, the largest peak detected was that associated with Compound 20 of parent mass  $m/z$  336 eluted here at 18.5 min. Compound 20 is the predominant peak in the particle phase extract but was also detected to a minor degree in the gas phase. This compound was the largest peak in all experiments conducted in this study either involving the presence of  $\text{NO}_x$ ,  $\text{H}_2\text{O}_2$  or  $\text{SO}_2$ .

Figure 4 shows both the EI (top) and CI (bottom) mass spectra of compound 20-BSTFA derivative. The CI mass spectrum of this compound shows characteristic fragment ions at  $m/z$  231 ( $M^+ - 105$ ), 247 ( $M^+ - 89$ ), and 321 ( $M^+ - 15$ ), and adducts at  $M^+ + 1$ ,  $M^+ + 29$ , and  $M^+ + 41$ . These fragments and adducts are consistent with the presence of three (-OH) groups and a molecular weight of the derivatized compound ( $M_d$ ) of 336 dal (all masses, hereafter, given as daltons) and compound molecular weight ( $M_c$ ) of 120. In addition, the absence of an  $m/z$  219 ( $M^+ - 117$ ) peak suggests the absence of an organic acid group in the compound. The EI spectrum of compound 20 shows fragments at  $m/z$  73, 131, 231, 321, and 337 (Fig. 4a), again consistent with the presence of three (-OH) groups, giving an  $M_d$  of 336 and an  $M_c$  of 120. The

mass spectra of BSTFA derivatives of compound 20, erythrose, and 2-methylglyceric acid (2-MGA) are similar, but each compound elutes at a different retention time and has a fragmentation pattern sufficiently different from compound 20 to distinguish the individual compounds. This is readily seen from an examination of the mass spectrum of erythrose formed from the oxidation of 1,3-butadiene (Andove et al., 2006).

The interpretation of the fragmentation patterns of the BSTFA derivative in EI and CI modes is shown in Scheme 1. Fragment ions at  $m/z$  117, 131, 157, 205, 231, 247, and 321 in Scheme 1 are postulated to come from loss of one or more groups including (-CH<sub>3</sub>), (-TMSOH), (-CH<sub>3</sub>)<sub>4</sub>Si, (-116 u), and (-TMSO). The base peak at  $m/z$  131, for example, is possibly formed by a combined loss of (-TMSO) and (-116 u) groups from the molecular ion M<sup>+</sup>; elimination of (-TMSO) leading to the formation of a fragment at  $m/z$  247. Thus, compound 20 has been tentatively identified as 2,3-dihydroxyisopentanol (DHIP; see Table 2) also detected to a very minor degree in the gas phase (Fig. 2).

Figure 5 shows mass spectra in the EI (top) and CI (bottom) modes for two additional silylated compounds eluting at 25.5 and 26 min (Fig. 3, Peaks 42 and 46). The silylated derivative analyzed in CI mode shows fragments at  $m/z$  437 (M<sup>+</sup> - 15), 319 (M<sup>+</sup> - 133), and 335 (M<sup>+</sup> - 117), and generally weak adducts at M<sup>+</sup> + 1, M<sup>+</sup> + 29, and M<sup>+</sup> + 41. Fragmentation patterns of the silylated compound are similar in CI and EI modes and are consistent with the presence of four -OH groups, with a derivative MW of 452. This compound was the most oxygenated product detected in MBO and tentatively identified as 2,3-dihydroxy-2-methylsuccinic acid (or isomers) with a compound MW of 164. This compound has been also detected in particle phase in field samples (Edney et al., 2003) and from the photooxidation of toluene and 1,3,5-trimethylbenzene.

Although 2-methylthreitol and 2-methylerythritol are found to originate from isoprene oxidation, these compounds were also detected during the oxidation of MBO (Fig. 3; Peaks 36 and 38). However, 2-MGA, which is also seen in aerosol from isoprene photooxidation, is just barely detectable above the chromatographic background and may have been formed from a slight isoprene impurity in the MBO. Given the extremely

**SOA formation from  
the atmospheric  
oxidation of MBO**

M. Jaoui et al.

Title Page

Abstract

Introduction

Conclusions

References

Tables

Figures

⏪

⏩

◀

▶

Back

Close

Full Screen / Esc

Printer-friendly Version

Interactive Discussion



**SOA formation from  
the atmospheric  
oxidation of MBO**

M. Jaoui et al.

Title Page

Abstract

Introduction

Conclusions

References

Tables

Figures

◀

▶

◀

▶

Back

Close

Full Screen / Esc

Printer-friendly Version

Interactive Discussion



small abundance of 2-MGA in these laboratory samples, it is unlikely this compound from MBO contributes measurably to aerosol collected under ambient conditions, especially where DHIP is very low. Given this assumption, it is relatively easy to determine the origin of the methyltetrols in ambient samples by examining the co-presence of 2-MGA or DHIP.

Other compounds identified in the particle phase include oxalic acid, 3-hydroxy-2-oxo-isopentanol/2,3-dihydroxy-3-methylbutanal, 2,3-trihydroxy-3-methylbutanal, 2-hydroxy-2-methylpropanedioic acid, and 2,3-dihydroxy-2-methylbutanedihyde. While compound names have been provided, structural isomers having the same set of derivative adducts or fragments are also possible, and thus the names might be ambiguous.

SOA products from the BSTFA derivatization have been quantified in the MBO system using the ketopinic acid (KPA) calibration method (Jaoui et al., 2004, 2005), since authentic standards are not available for these compounds. By this technique, the integrated TIC of the compound of interest is determined against the TIC of KPA. The accuracy of this approach has previously been discussed and for an oxygenated diacid, such as pinic acid, has been found to be on the order of 60%. Compound abundances for DHIP, methyltetrols, and 2,3-dihydroxy-2-methylsuccinic acid were thus determined by this method for experiment, ER-462, ER-464, and ER465b as shown in Fig. 6. Concentrations of  $52 \mu\text{g m}^{-3}$  have been determined for DHIP.

### 3.4 Field measurements

The gas phase organic compounds were observed in laboratory samples are also present in ambient air. High concentrations of formaldehyde, glyoxal, methylglyoxal, acetaldehyde, acetone, and oxalic acid were observed from MBO oxidation. Data reported in the literature shows that these compounds are ubiquitous in ambient samples and suggests that MBO might be a source of these compounds in areas dominated by trees having high MBO emission rates. In addition, the uptake of some of these compounds (e.g., glyoxal, methylglyoxal) in the aerosol phase followed by heterogeneous

sulfur chemistry can lead to SOA formation (Carlton et al., 2007; Liggió et al., 2005). Recently, Steiner et al. (2007) showed that MBO oxidation causes an increase in ambient ozone, formaldehyde, acetone, and hydroxyl radicals, which can increase the oxidant capacity and chemical reactivity of the atmosphere.

Of greater interest for this work are compounds seen in the present work that might be found in ambient PM<sub>2.5</sub>. 2-Methylthreitol and 2-methylerythritol observed previously in ambient PM<sub>2.5</sub> and has thought to have been produced only from the photooxidation of isoprene. From this work, it now appears that the methyltetrols might also have been generated in the atmosphere from the photooxidation of MBO. Additionally, 2,3-dihydroxy-2-methylsuccinic acid observed in this study has been previously reported in ambient PM<sub>2.5</sub> samples (Edney et al., 2003) but appears to be produced as well during the photooxidation of toluene and 1,3,5-trimethylbenzene. Of the particle phase compounds which have been detected from the photooxidation of MBO, it appears that only DHIP is unique to this precursor. In fact, in selected ambient samples, particularly those collected in a forested environment, DHIP have been detected in this study. Although, DHIP was detected in several field samples analyzed by our group (e.g., CMAPS field study (Kleindienst et al., 2011); Midwestern United States (Lewandowski et al., 2007a, b)), the field samples analyzed for this paper focus on samples collected from a 2006 field study at Duke Forest, NC. A comparison of a mass spectrum from the laboratory sample with that measured at the field site is shown in Fig. 7. Using the KPA method described above, estimates for ambient concentrations for DHIP are then made and shown in Fig. 8. The average concentrations of DHIP ranged from 0.1 during winter season to ~1 ng m<sup>-3</sup> during summer season.

Finally, adapting an organic tracer method developed by Kleindienst et al. (2007), a mass fraction of DHIP was measured and used to estimate the SOA contribution from MBO to ambient organic aerosol. For this determination, the collected chamber SOA was analyzed for OC and DHIP, and organic aerosol mass fraction was calculated as described by Kleindienst et al. (2007). An SOA to SOC ratio (SOA/SOC) of 2 was obtained for MBO SOA. Based on experiments ER-464, an average value of aerosol mass

## SOA formation from the atmospheric oxidation of MBO

M. Jaoui et al.

Title Page

Abstract

Introduction

Conclusions

References

Tables

Figures

⏪

⏩

◀

▶

Back

Close

Full Screen / Esc

Printer-friendly Version

Interactive Discussion



fraction was 0.05 (C/C). Next the concentration of the tracer compound was measured in a series of ambient samples from a forested area in NC. 2,3-Dihydroxyisopentanol was detected mainly during the warmest seasons when MBO emissions were high.

#### 4 Summary

Several recent advances have been made in organic aerosol research, and new precursors to SOA are being identified. Although the chemical characteristics of gas-phase reaction products formed from MBO oxidation have been widely studied, relatively few particulate phase reaction products have been reported, and MBO is generally believed to contribute little to ambient organic aerosol. In the present study, laboratory experiments have been carried out to investigate SOA formation from the oxidation of MBO in the presence and absence of  $\text{NO}_x$ , and/or  $\text{H}_2\text{O}_2$ ,  $\text{SO}_2$ . SOA collected under these conditions have been analyzed for organic carbon and organic reaction products using OC/EC analysis and gas chromatography/mass spectrometry, respectively. The resulting analyses showed the presence of a large number of oxygenated organic compounds in the gas and filter extracts.

To determine the relative contributions to ambient aerosol of SOA products formed from MBO,  $\text{PM}_{2.5}$  samples were BSTFA derivatized and GC-MS analyzed. Emphasis was placed on polar oxygenated organic compounds. A series of organic compounds were found in both ambient  $\text{PM}_{2.5}$  and chamber SOA, but most of these compounds were detected in SOA originating from several hydrocarbon precursors previously studied in our laboratory. 2,3-Dihydroxyisopentanol, however, was detected only in SOA produced from MBO oxidation. This compound is further studied to determine its viability to serve as an MBO organic tracer in atmospheric particulate matter. It was found to be dependent on both the degree of aerosol acidity and MBO levels in ambient  $\text{PM}_{2.5}$  samples.

### SOA formation from the atmospheric oxidation of MBO

M. Jaoui et al.

Title Page

Abstract

Introduction

Conclusions

References

Tables

Figures

◀

▶

◀

▶

Back

Close

Full Screen / Esc

Printer-friendly Version

Interactive Discussion





**SOA formation from  
the atmospheric  
oxidation of MBO**

M. Jaoui et al.

Title Page

Abstract

Introduction

Conclusions

References

Tables

Figures

◀

▶

◀

▶

Back

Close

Full Screen / Esc

Printer-friendly Version

Interactive Discussion



Environ., 33, 2893–2905, 1999.

Andove, D. E., Fookes, C. J. R., Hynes, R. G., Walters, C. K., and Azzi, A.: The characterization of secondary organic aerosol formed during the photooxidation of 1,3-butadiene in air containing nitric oxide, *Atmos. Environ.*, 40, 4597–4607, 2006.

5 Atkinson, R.: Atmospheric chemistry of VOCs and NO<sub>x</sub>, *Atmos. Environ.*, 2063–2101, 2000.

Baker, B., Guenther, A., Greenberg, J., Goldstein, A., and Fall, R.: Canopy fluxes of 2-methyl-3-buten-2-ol over a ponderosa pine forest by relaxed eddy accumulation: Field data and model comparison, *J. Geophys. Res.*, D, 104, 26107–26114, 1999.

10 Blunden, J., Aneja, V. P., and Lonneman, W. A.: Characterization of non-methane volatile organic compounds at swine facilities in eastern North Carolina, *Atmos. Environ.*, 39, 6707–6718, 2005.

Carlton, A. G., Turpin, B. J., Altieri, K. E., Seitzinger, S., Reff, A., Lim, H.-J., and Ervens, B.: Atmospheric oxalic acid and SOA production from glyoxal: Results of aqueous photooxidation experiments, *Atmos. Environ.*, 41, 7588–7602, 2007.

15 Carrasco, N., Doussin, J. F., O'Connor, M., Wenger, J. C., Picquet-Varrault, B., Durand-Jolibois, R., and Carlier, P.: Simulation chamber studies of the atmospheric oxidation of 2-methyl-3-buten-2-ol: Reaction with hydroxyl radicals and ozone under a variety of conditions, *J. Atmos. Chem.*, 56, 33–55, 2007.

20 Chan, A. W., Galloway, M. M., Kwan, A. J., Chabra, P. S., Keutsch, F. N., Wennberg, P. O., Flanagan, R. C., and Seinfeld, J. H.: Photooxidation of 2-methyl-3-buten-2-ol (MBO) as a potential source of secondary organic aerosol, *Environ Sci. Technol.*, 43(13), 4647–1652, 2009.

Charlson, R. J., Schwartz, S. E., Hales, J. M., Cess, R. D., Coakley Jr., J. A., Hansen, J. E., and Hoffman, D. J.: Climate forcing by anthropogenic aerosols, *Science*, 255, 423–430, doi:10.1126/science.255.5043.423, 1992.

25 Edney, E. O., Kleindienst, T. E., Conner, T. S., McIver, C. D., Corse, E. W., and Weathers, W. S.: Polar organic oxygenates in PM<sub>2.5</sub> at a southeastern site in the United States, *Atmos. Environ.*, 37, 3947–3956, 2003.

Fantechi, G., Jensen, N. R., Hjorth, J., and Peeters, J.: Mechanistic studies of the atmospheric oxidation of methylbutenol by OH radicals, ozone and NO<sub>3</sub> radicals, *Atmos. Environ.*, 32, 3547–3556, 1998.

30 Geron, C. D. and Arnts, R. R.: Seasonal monoterpene and sesquiterpene emissions from *Pinus taeda* and *Pinus virginiana*, *Atmos. Environ.*, 44, 4240–4251, 2010.

Goldan, P. D., Kuster, W. C., and Fehsenfeld, F. C.: The observation of a C<sub>5</sub> alcohol emission

**SOA formation from  
the atmospheric  
oxidation of MBO**

M. Jaoui et al.

[Title Page](#)[Abstract](#)[Introduction](#)[Conclusions](#)[References](#)[Tables](#)[Figures](#)[◀](#)[▶](#)[◀](#)[▶](#)[Back](#)[Close](#)[Full Screen / Esc](#)[Printer-friendly Version](#)[Interactive Discussion](#)

in a North American pine forest, *Geophys. Res. Lett.*, 20, 1039–1042, 1993.

Gray, D. W.: Transient increase in methylbutenol emission following partial defoliation of *Pinus ponderosa*, *Atmos. Environ.*, 42, 4797–4802, 2008.

Grosjean, D. and Grosjean, E.: Carbonyl products of the ozone-unsaturated alcohol reaction, *J. Geophys. Res.*, 100(D11), 22815–22820, 1995.

Guenther, A., Hewitt, C. N., Erickson, D., Fall, R., Geron, C., Graedel, T., Harley, P., Klinger, L., Lerdau, M., McKay, W. A., Pierce, T., Scholes, B., Steinbrecher, R., Tallamraju, R., Taylor, T., and Zimmerman, P.: A global model of natural volatile organic compound emissions, *J. Geophys. Res.-Atmos.*, 100, 8873–8892, 1995.

Guenther, A., Karl, T., Harley, P., Wiedinmyer, C., Palmer, P. I., and Geron, C.: Estimates of global terrestrial isoprene emissions using MEGAN (Model of Emissions of Gases and Aerosols from Nature), *Atmos. Chem. Phys.*, 6, 3181–3210, doi:10.5194/acp-6-3181-2006, 2006.

Harley, P., Fridd-Stroud, V., Greenberg, J., Guenther, A., Vasconcellos, P.: Emission of 2-methyl-3-buten-2-ol by pines: a potentially large natural source of reactive carbon to the atmosphere, *J. Geophys. Res.*, 103, 25479–25486, 1998.

Jaoui, M., Kleindienst, T. E., Lewandowski, M., and Edney, E. O.: Identification and quantification of aerosol polar oxygenated compounds bearing carboxylic and/or hydroxyl groups. 1. Method development, *Anal. Chem.*, 76, 4765–4778, 2004.

Jaoui, M., Kleindienst, T. E., Lewandowski, M., Offenberg, J. H., and Edney, E. O.: Identification and quantification of aerosol polar oxygenated compounds bearing carboxylic or hydroxyl groups. 2. Organic tracer compounds from monoterpenes, *Environ. Sci. Technol.*, 39, 5661–5673, 2005.

Jaoui, M., Corse, E. W., Lewandowski, M., Offenberg, J. H., Kleindienst, T. E., and Edney, E. O.: Formation of organic tracers for isoprene SOA under acidic conditions, *Atmos. Environ.*, 44, 1798–1805, 2010.

Jayne, J. T., Leard, D. C., Zhang, X., Davidovits, P., Smith, K. A., Kolb, C. E., and Worsnop, D. R.: Development of an Aerosol Mass Spectrometer for Size and Composition. Analysis of Submicron Particles, *Aerosol Sci. Technol.*, 33, 49–70, 2000.

Kanakidou, M., Seinfeld, J. H., Pandis, S. N., Barnes, I., Dentener, F. J., Facchini, M. C., Van Dingenen, R., Ervens, B., Nenes, A., Nielsen, C. J., Swietlicki, E., Putaud, J. P., Balkanski, Y., Fuzzi, S., Horth, J., Moortgat, G. K., Winterhalter, R., Myhre, C. E. L., Tsigaridis, K., Vignati, E., Stephanou, E. G., and Wilson, J.: Organic aerosol and global climate modelling:

**SOA formation from  
the atmospheric  
oxidation of MBO**

M. Jaoui et al.

Title Page

Abstract

Introduction

Conclusions

References

Tables

Figures

◀

▶

◀

▶

Back

Close

Full Screen / Esc

Printer-friendly Version

Interactive Discussion



a review, *Atmos. Chem. Phys.*, 5, 1053–1123, doi:10.5194/acp-5-1053-2005, 2005.

Kim, S., Karl, T., Guenther, A., Tyndall, G., Orlando, J., Harley, P., Rasmussen, R., and Apel, E.: Emissions and ambient distributions of Biogenic Volatile Organic Compounds (BVOC) in a ponderosa pine ecosystem: interpretation of PTR-MS mass spectra, *Atmos. Chem. Phys.*, 10, 1759–1771, doi:10.5194/acp-10-1759-2010, 2010.

Kleindienst, T. E., Edney, E. O., Lewandowski, M., Offenberg, J. H., and Jaoui, M.: Secondary organic carbon and aerosol yields from the irradiations of isoprene and  $\alpha$ -pinene in the presence of  $\text{NO}_x$  and  $\text{SO}_2$ , *Environ. Sci. Technol.*, 40, 3807–3812, 2006.

Kleindienst, T. E., Jaoui, M., Lewandowski, M., Offenberg, J. H., Lewis, C. W., Bhave, P. V., and Edney, E. O.: Estimates of the contributions of biogenic and anthropogenic hydrocarbons to secondary organic aerosol at a southeastern US location, *Atmos. Environ.*, 41, 8288–8300, 2007.

Kleindienst, T. E., Lewandowski, M., Offenberg, J. H., Jaoui, M., and Edney, E. O.: The formation of secondary organic aerosol from the isoprene + OH reaction in the absence of  $\text{NO}_x$ , *Atmos. Chem. Phys.*, 9, 6541–6558, doi:10.5194/acp-9-6541-2009, 2009.

Kleindienst, T. E., Lewandowski, M., Offenberg, J. H., Jaoui, M., Edney, E. O., Zheng, M., and Ding, X.: Contribution of primary and secondary sources to organic aerosol and  $\text{PM}_{2.5}$  at SEARCH Network Sites, *Air Waste Manage. Assoc.*, 60, 1388–1399, 2010.

Kleindienst, T. E., Offenberg, J. H., Lewandowski, M., Piletic, I., Jaoui, M., Lee, A., Bohnenkamp, C., Hoag, K., Rubitschun, C. L., and Surratt, J. D.: Secondary Organic Aerosol Contributions during CalNex – Bakersfield, CALNEX workshop, CA, 2011.

König, G., Brunda, M., Pauxbaum, H., Hewitt, C. N., Duckham, S. C., and Rudolph, J.: Relative contribution of oxygenated hydrocarbons to the total biogenic VOC emissions of selected mid-European agricultural and natural plant species, *Atmos. Environ.*, 29, 861–874, 1995.

Kroll, J. H., Ng, N. L., Murphy, S. M., Varutbangkul, V., Flagan, R. C., and Seinfeld, J. H.: Chamber studies of secondary organic aerosol growth by reactive uptake of simple carbonyl compounds, *J. Geophys. Res.*, 110, D23207, doi:10.1029/2005JD006004, 2005.

Lamanna, M. S. and Goldstein, A. H.: In situ measurements of C2-C10 volatile organic compounds above a Sierra Nevada ponderosa pine plantation, *J. Geophys. Res.*, 104(D17), 21247–21262, 1999.

Lewandowski, M., Jaoui, M., Kleindienst, T. E., Offenberg, J. H., and Edney, E. O.: Composition of  $\text{PM}_{2.5}$  during the summer of 2003 in Research Triangle Park, North Carolina, *Atmos. Environ.*, 41(19), 4073–4083, 2007a.

**SOA formation from  
the atmospheric  
oxidation of MBO**

M. Jaoui et al.

Title Page

Abstract

Introduction

Conclusions

References

Tables

Figures

◀

▶

◀

▶

Back

Close

Full Screen / Esc

Printer-friendly Version

Interactive Discussion



- Lewandowski, M., Jaoui, M., Offenber, J. H., Kleindienst, T. E., Edney, E. O., Sheesley, R. J., and Schauer, J. J.: Primary and secondary contributions to ambient PM<sub>2.5</sub> in the Midwestern United States, *Environ. Sci. Technol.*, 42, 3303–3309, 2007b.
- Liggio, J., Li, S. M., and McLaren, R.: Reactive uptake of glyoxal by particulate matter, *J. Geophys. Res.*, 110, D10304, doi:10.1029/2004JD005113, 2005.
- Noda, J. and Ljungstrom, E.: Aerosol formation in connection with NO<sub>3</sub> oxidation of unsaturated alcohols, *Atmos. Environ.*, 36, 521–525, 2002.
- Offenber, J. H., Kleindienst, T. E., Jaoui, M., Lewandowski, M., and Edney, E. O.: Thermal properties of secondary organic aerosol, *Geophys. Res. Lett.*, 33, L03816, doi:10.1029/2005GL024623, 2006.
- Pope III, C. A., Ezzati, M., and Dockery, D. W.: Fine particulate air pollution and life expectancy in the United States, *N. Eng. J. Med.*, 360(4), 376–386, 2009.
- Schwartz, J., Dockery, D. W., and Neas, L. M.: Is daily mortality associated specifically with fine particles, *J. Air Waste Manage. Assoc.*, 46, 929–939, 1996.
- Sisler, J. F. and Malm, W. C.: The Relative importance of soluble aerosols to spatial and seasonal trends of impaired visibility in the United States, *Atmos. Environ.*, 28, 851–862, 1994.
- Smith, D. F., Kleindienst, T. E., Hudgens, E. E., and Bufalini, J.: Measurement of organic atmospheric transformation products by gas chromatography, *J. Chromatogr.*, 54, 265–281, 1989.
- Spaulding, R. S. and Charles, M. J.: Comparison of methods for extraction, storage and silylation of pentafluorobenzyl derivatives of carbonyl compounds and multifunctional carbonyl compounds, *Anal. Bioanal. Chem.*, 372, 808–816, 2002.
- Spaulding, R. S., Schade, G. W., Goldstein, A. H., and Charles, M. J.: Characterization of secondary atmospheric photooxidation products: Evidence for biogenic and anthropogenic sources, *J. Geophys. Res.*, 108(D8), 4247, doi:10.1029/2002JD002478, 2003.
- Steiner, A. L., Tonse, S., Cohen, R. C., Goldstein, A. H., and Harley, R. A.: Biogenic 2-methyl-3-buten-2-ol increases regional ozone and HO<sub>x</sub> sources, *Geophys. Res. Lett.*, 34, L15806, doi:10.1029/2007GL030802, 2007.
- Tarvainen, V., Hakola, H., Hellén, H., Bäck, J., Hari, P., and Kulmala, M.: Temperature and light dependence of the VOC emissions of Scots pine, *Atmos. Chem. Phys.*, 5, 989–998, doi:10.5194/acp-5-989-2005, 2005.
- Volkamer, R., San Martini, F., Molina, L. T., Salcedo, D., Jimenez, J. L., and Molina, M. J.: A missing sink for gas-phase glyoxal in Mexico City: Formation of secondary organic aerosol,

---

**SOA formation from  
the atmospheric  
oxidation of MBO**

M. Jaoui et al.

---

Title Page

Abstract

Introduction

Conclusions

References

Tables

Figures



Back

Close

Full Screen / Esc

Printer-friendly Version

Interactive Discussion



## SOA formation from the atmospheric oxidation of MBO

M. Jaoui et al.

**Table 1.** Initial conditions for MBO experiments in the presence and absence of NO.

Exp. ID <sup>a</sup>	MBO (ppm C)	H <sub>2</sub> O <sub>2</sub> (ppm)	CH <sub>3</sub> ONO (ppm)	NO (ppm)	SO <sub>2</sub> (ppm)	T (°C)	RH (%)
ER <sup>st</sup> -462	19.0	18.8	–	–	–	21	<3
ER <sup>st</sup> -463	14.6	–	–	0.288	–	23	30
ER <sup>dy</sup> -464a	18.2	6.6	–	–	–	24	<3
ER <sup>dy</sup> -464b	18.2	6.6	–	–	0.210	24	<3
ER <sup>dy</sup> -465a	16.4	–	0.287	0.285	–	26	30
ER <sup>dy</sup> -465b	15.1	–	0.279	0.245	0.212	26	30
ER <sup>st</sup> -567	15.4	–	–	0.309	–	22	28

<sup>dy</sup>: dynamic (flow-mode) experiments; <sup>st</sup>: static (batch-mode) experiments.

Title Page

Abstract

Introduction

Conclusions

References

Tables

Figures

◀

▶

◀

▶

Back

Close

Full Screen / Esc

Printer-friendly Version

Interactive Discussion



**Table 2.** SOA and gas phase compounds identified in the present study. Particle phase MW of the BSTFA is given, for gas phase the MW of the underivatized compound is given.

ID	Rt (min)	MW (amu)	<i>m/z</i> (methane-Cl) BSTFA or PFBHA+BSTFA derivative	Tentative ID
Particle phase				
1	11.19	248 <sub>d</sub>	205(100), 233, 131, 73, 249	–
2	11.74	315	73(100), 300, 316, 344, 356	–
3	11.85	–	233(100), 73, 233, 159, 247	–
4	12.34	–	231(100), 73, 245, 157, 289	–
5	13.11	–	168(100), 196, 208, 96, 73	–
6	13.38	174	159(100), 73, 80, 175, 203	–
7	13.65	–	242(100), 73, 300, 411, 427	–
8	13.89	–	315(100), 389, 227, 343, 73	Sulfuric acid/Ammonium sulfate
9	14.09	–	207(100), 80, 73, 322, 295	–
10	14.20	–	406(100), 390, 420, 221, 73	–
11	14.29	–	73(100), 189, 117, 233, 249	–
12	14.66	–	221(100), 390, 73, 406, 336	–
13	14.84	–	73(100), 316, 332, 177, 221	–
14	14.97	–	73(100), 277, 131, 189, 247	–
15	15.93	–	73(100), 179, 265, 293, 59	–
16	16.26	348	73(100), 131, 189, 277, 349	–
17	16.59	–	196(100), 180, 73, 73, 247	–
18	17.34	–	374(100), 73, 189, 389, 284	–
19	17.50	–	73(100), 131, 173, 189, 247	–
20	18.29	336	231(100), 247, 157, 191, 321	2,3-Dihydroxyisopentanol
21	18.45	334	319(100), 334, 229, 245, 73	3-Hydroxy-2-oxoisopentanol
22	18.83	–	73(100), 221, 281, 330, 443	–
23	18.92	–	73(100), 430, 272, 217, 386	–
24	19.34	350	73(100), 189, 205, 247, 117	1,2,3-trihydroxy-3-methylbutanal

## SOA formation from the atmospheric oxidation of MBO

M. Jaoui et al.

Title Page

Abstract

Introduction

Conclusions

References

Tables

Figures

◀

▶

◀

▶

Back

Close

Full Screen / Esc

Printer-friendly Version

Interactive Discussion



**Table 2.** Continued.

ID	Rt (min)	MW (amu)	<i>m/z</i> (methane-Cl) BSTFA or PFBHA+BSTFA derivative	Tentative ID
25	19.79	350	217(100), 335, 73, 277, 291	2-hydroxy-2-methylpropanedioic acid
26	20.8	313	298(100), 73, 221, 268, 342	–
27	20.75	–	159(100), 73, 117, 175, 247	–
28	20.86	–	159(100), 73, 117, 175, 247	–
29	21.51	–	159(100), 73, 117, 175, 247	–
30	21.64	–	238(100), 159, 222, 73, 142	–
31	22.05	–	73(100), 231, 157, 191, 247	–
32	22.18	–	73(100), 231, 157, 191, 247	–
33	22.30	–	296(100), 206, 132, 222, 312	–
34	22.68	254	165(100), 239, 255, 283, 295	Ketopinic acid (IS)
35	23.27	424	409(100), 219, 319, 293, 203	2-methylerythritol
36	23.41	–	205(100), 73, 265, 221, 131	–
37	23.54	–	73(100), 201, 275, 175, 80	–
38	23.73	424	409(100), 219, 319, 293, 203	2-methylthreitol
39	24.88	276	73(100), 131, 191, 205, 261	2,3-dihydroxy-2-methylbutane di-aldehyde
40	25.23	–	73(100), 219, 117, 231, 189	–
41	25.31	–	73(100), 231, 159, 205, 305	–
42	25.40	–	73(100), 231, 159, 205, 305	–
43	25.49	–	73(100), 131, 191, 291, 215	–
44	25.67	452	437(100), 319, 335, 203, 481	2,3-dihydroxy-2-methylsuccinic acid and isomers
45	25.81	–	73(100), 131, 191, 291, 215	–
46	25.97	452	437(100), 319, 335, 203, 481	2,3-dihydroxy-2-methylsuccinic acid and isomers
47	26.13	–	73(100), 231, 157, 177, 247	–
48	26.40	–	205(100), 73, 231, 333, 407	–

**SOA formation from the atmospheric oxidation of MBO**

M. Jaoui et al.

Title Page

Abstract

Introduction

Conclusions

References

Tables

Figures

◀

▶

◀

▶

Back

Close

Full Screen / Esc

Printer-friendly Version

Interactive Discussion



**Table 2.** Continued.

ID	Rt (min)	MW (amu)	<i>m/z</i> (methane-Cl) BSTFA or PFBHA+BSTFA derivative	Tentative ID
49	26.98	–	157(100), 73, 231, 247, 379	–
50	27.07	–	73(100), 275, 335, 393, 177	–
51	27.58	–	73(100), 231, 117, 205, 293	–
52	28.01	–	73(100), 157, 247, 219, 131	–
Gas phase				
53	–	30	–	Formaldehyde
54	–	44	–	acetaldehyde
55	–	58	–	acetone
56	31.08	58	449(100), 181, 477, 489, 521	glyoxal
57	–	60	–	glycolaldehyde
58	31.71	72	463(100), 491, 181, 445, 265	methylglyoxal
59	22.71	74	342(100), 382, 326, 73, 370	glyoxylic acid
60	32.06	86	477(100), 181, 505, 279, 459	2,3-butanedione
61	38.19	86	672(100), 700, 181, 642, 111	2-oxopropane-1,3-dial
62	25.50	88	266(100), 310, 338, 181, 364	2-hydroxy-2-methylpropanal
63	33.80	88	563(100), 291, 251, 489, 181	2-hydroxypropane-1,3-dial
65	37.48	100	686(100), 488, 714, 181, 776	2,3-dioxobutanal
66	34.55	114	505(100), 266, 181, 533, 545	2,3-dioxobutane-1,4-dial
*	27.53	118	442(100), 73, 368, 294, 486	3-hydroxy-2-oxo-isopentanol
*	27.82	118	442(100), 352, 368, 233, 73	2,3-dihydroxy-3-methylbutanal
67	35.57	132	593(100), 503, 536, 621, 354	2,3-dihydroxy-2-methylbutane di-aldehyde
68	26.73	116	294(100), 368, 384, 412, 73	2-Oxovaleric acid

**SOA formation from the atmospheric oxidation of MBO**

M. Jaoui et al.

Title Page

Abstract

Introduction

Conclusions

References

Tables

Figures



Back

Close

Full Screen / Esc

Printer-friendly Version

Interactive Discussion



## SOA formation from the atmospheric oxidation of MBO

M. Jaoui et al.

**Table 3.** OM/OC ratio and SOA and SOC yields. Note in experiment ER-464a, the aerosol mass concentration is SOA mass concentration, and in Experiments ER-464b and ER-465b the aerosol mass concentration is a mixture of SOA and inorganic sulfate compounds originated from SO<sub>2</sub> reaction.

Exp. ID	Reacted MBO ( $\mu\text{g m}^{-3}$ )	Reacted MBO ( $\mu\text{g C m}^{-3}$ )	Aerosol ( $\mu\text{g m}^{-3}$ )	SOC ( $\mu\text{g C m}^{-3}$ )	OM/OC	$Y_{\text{SOA}}$ (%)	$Y_{\text{SOC}}$ (%)
ER-464a	4967	3465	32.5	15.5	2.1	0.7	0.5
ER-464b	5994	4182	74.1	37.6	–	–	0.9
ER-465b	10 623	7411	138.0	12.3	–	–	0.2

Title Page

Abstract

Introduction

Conclusions

References

Tables

Figures

◀

▶

◀

▶

Back

Close

Full Screen / Esc

Printer-friendly Version

Interactive Discussion



SOA formation from  
the atmospheric  
oxidation of MBO

M. Jaoui et al.

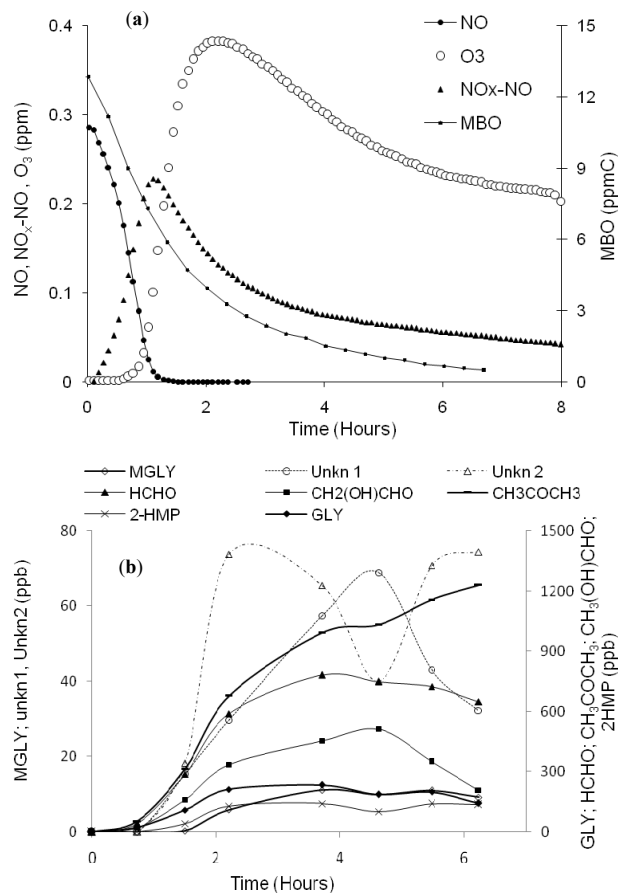


**Fig. 1.** Time profiles of gas phase oxidation products from the oxidation of MBO. **(a)** Experiment ER-463; **(b)** experiment ER-467.

SOA formation from  
the atmospheric  
oxidation of MBO

M. Jaoui et al.

Title Page

Abstract

Introduction

Conclusions

References

Tables

Figures

◀

▶

◀

▶

Back

Close

Full Screen / Esc

Printer-friendly Version

Interactive Discussion

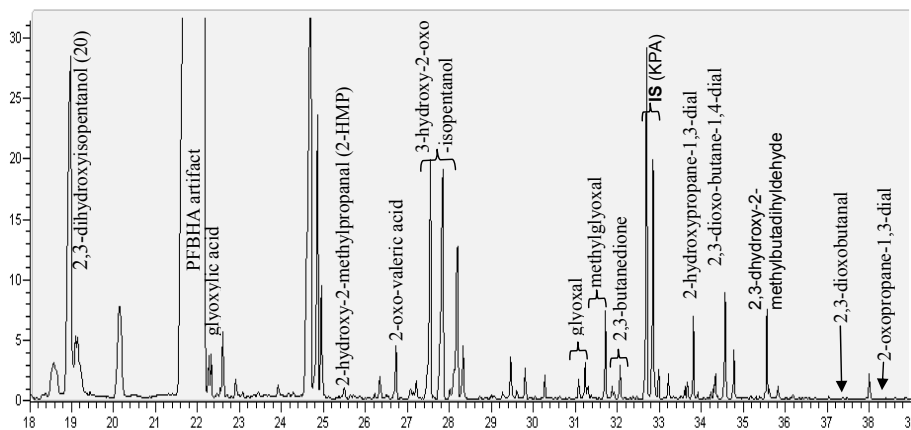


**Fig. 2.** GC-MS total ion current (TIC) chromatograms of organic extract as PFBHA + BSTFA (gas phase) derivatives from an irradiated MBO.

SOA formation from  
the atmospheric  
oxidation of MBO

M. Jaoui et al.

Title Page

Abstract

Introduction

Conclusions

References

Tables

Figures

◀

▶

◀

▶

Back

Close

Full Screen / Esc

Printer-friendly Version

Interactive Discussion

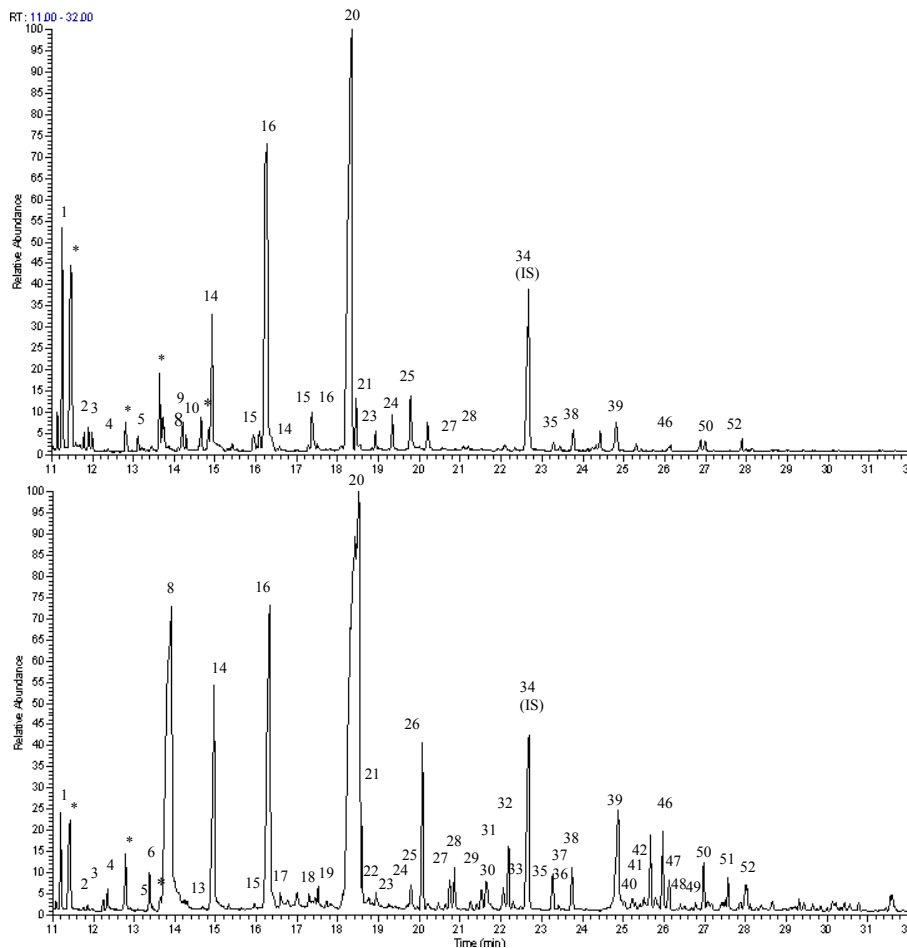


**Fig. 3.** GC-MS total ion current chromatogram of organic extracts as BSTFA derivatives for particle phase products from the photooxidation of MBO in the absence (top) and presence (bottom) of acidic sulfate aerosol.

SOA formation from  
the atmospheric  
oxidation of MBO

M. Jaoui et al.

Title Page

Abstract

Introduction

Conclusions

References

Tables

Figures



Back

Close

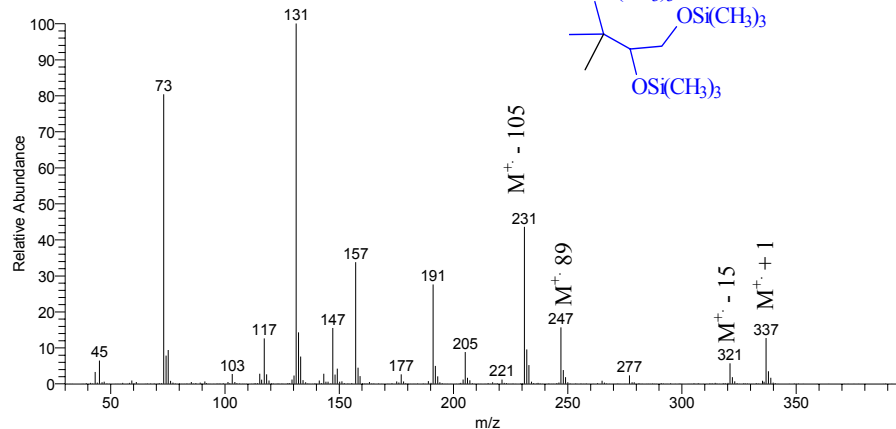
Full Screen / Esc

Printer-friendly Version

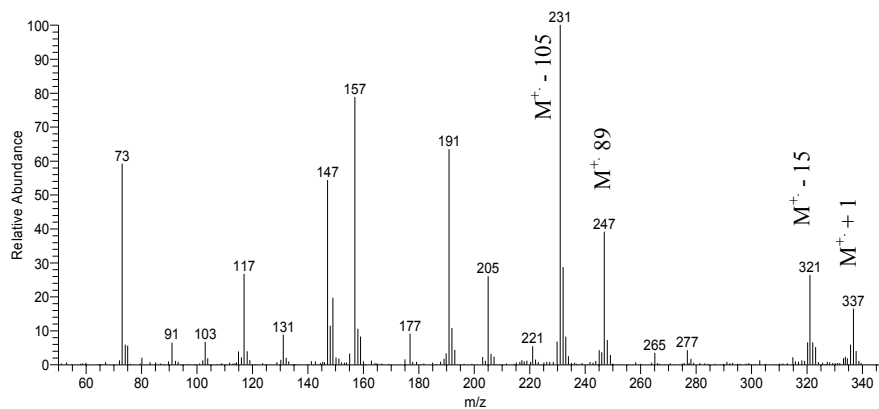
Interactive Discussion



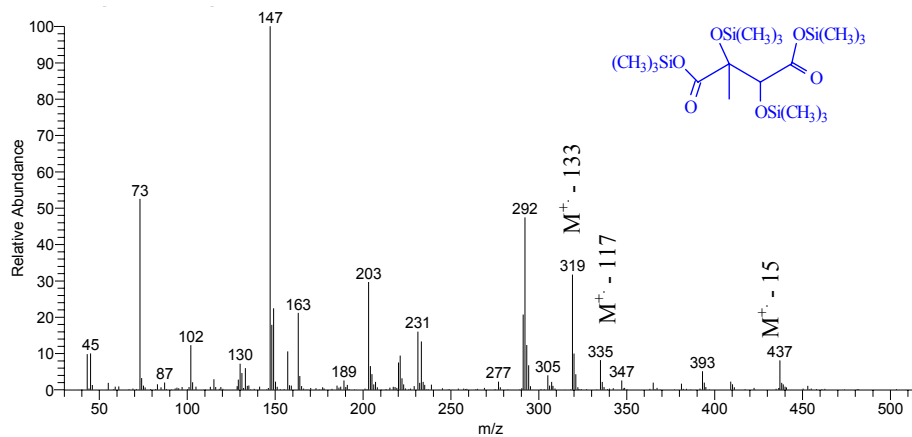
(a): 2,3-dihydroxyisopentanol (20: DHIP) (EI mode)



(b): 2,3-dihydroxyisopentanol (20: DHIP) (CI mode)

**Fig. 4.** EI (a) and CI (b) mass spectra of the BSTFA derivative of 2,3-dihydroxyisopentanol (20).

(a) EI mode



(b) CI mode

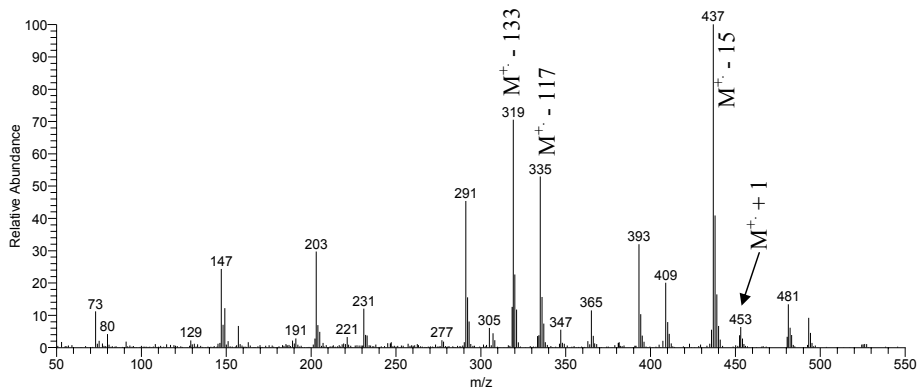


**Fig. 5.** Mass spectra of (42 and 46 from Fig. 3) tentatively identified as 2,3-dihydroxy-2-methylsuccinic acid.

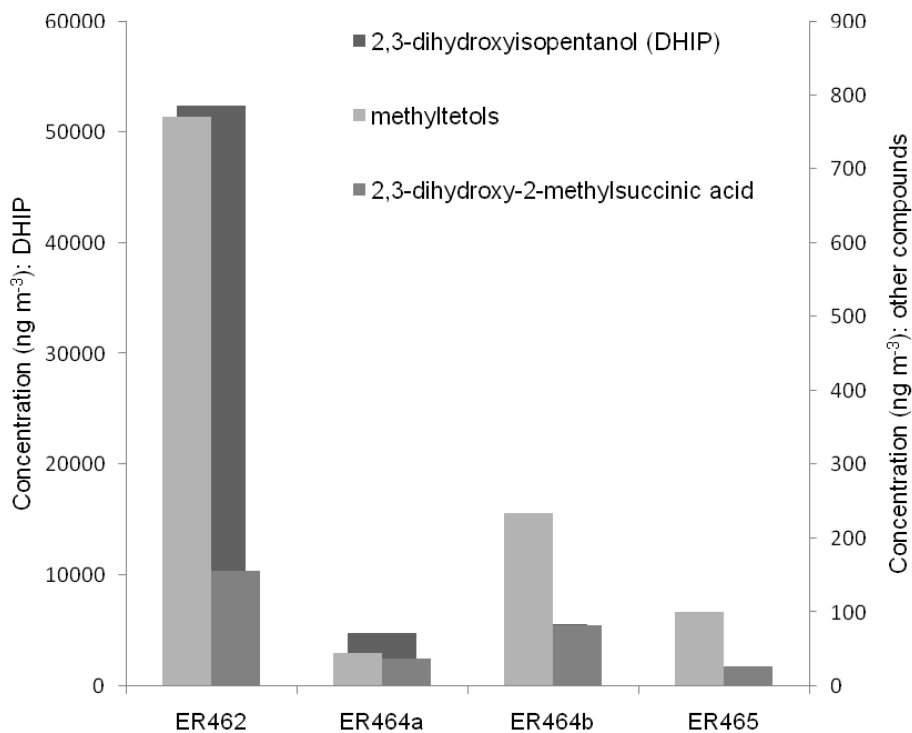


**Fig. 6.** Concentrations (ng m<sup>-3</sup>) of DHIP, methyltetrols (2-methylerythritol + 2-methylthreitol), and 2,3-dihydroxy-2-methylsuccinic acid as KPA.

**SOA formation from the atmospheric oxidation of MBO**

M. Jaoui et al.

Title Page

Abstract Introduction

Conclusions References

Tables Figures

◀ ▶

◀ ▶

Back Close

Full Screen / Esc

Printer-friendly Version

Interactive Discussion



SOA formation from  
the atmospheric  
oxidation of MBO

M. Jaoui et al.

Title Page

Abstract

Introduction

Conclusions

References

Tables

Figures

◀

▶

◀

▶

Back

Close

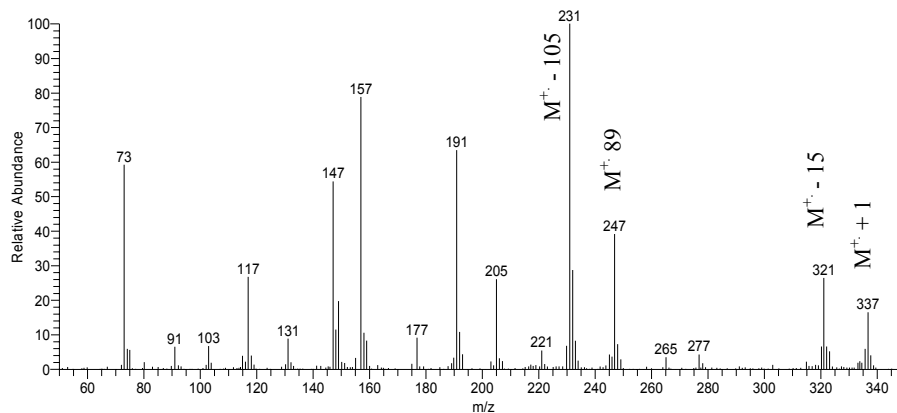
Full Screen / Esc

Printer-friendly Version

Interactive Discussion



(a): DHIP (20) in chamber experiment (CI mode)



(b): DHIP (20) in ambient samples (CI mode)

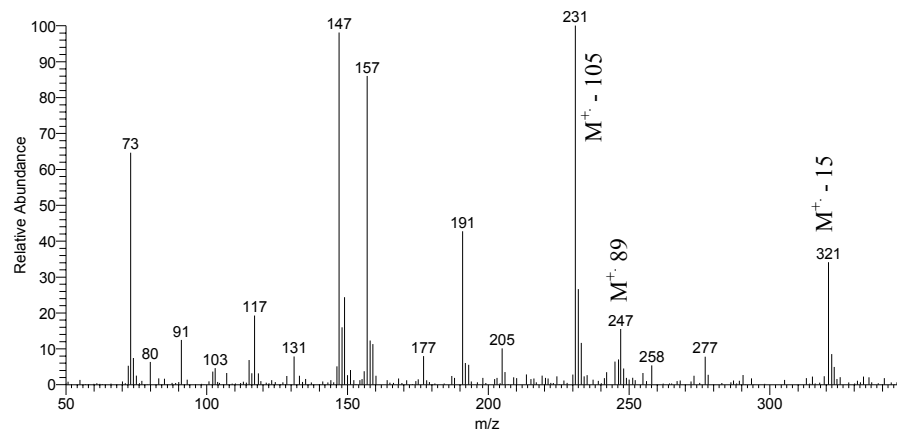


**Fig. 7.** Mass spectrum of the BSTFA derivative of DHIP (20) in CI mode observed in chamber experiment (a), and ambient samples (b).

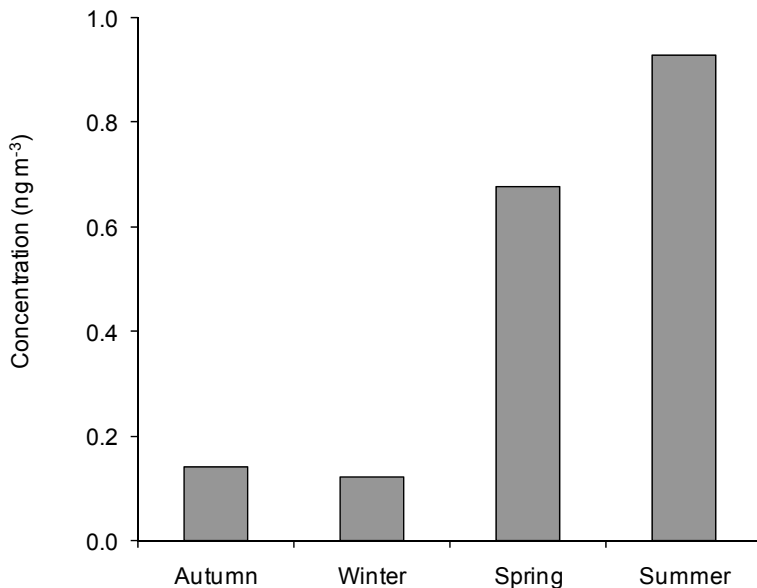


**Fig. 8.** Ambient concentrations of MBO tracer DHIP measured during 2006 campaign at Duke Forest NC.

**SOA formation from the atmospheric oxidation of MBO**

M. Jaoui et al.

Title Page

Abstract Introduction

Conclusions References

Tables Figures

◀ ▶

◀ ▶

Back Close

Full Screen / Esc

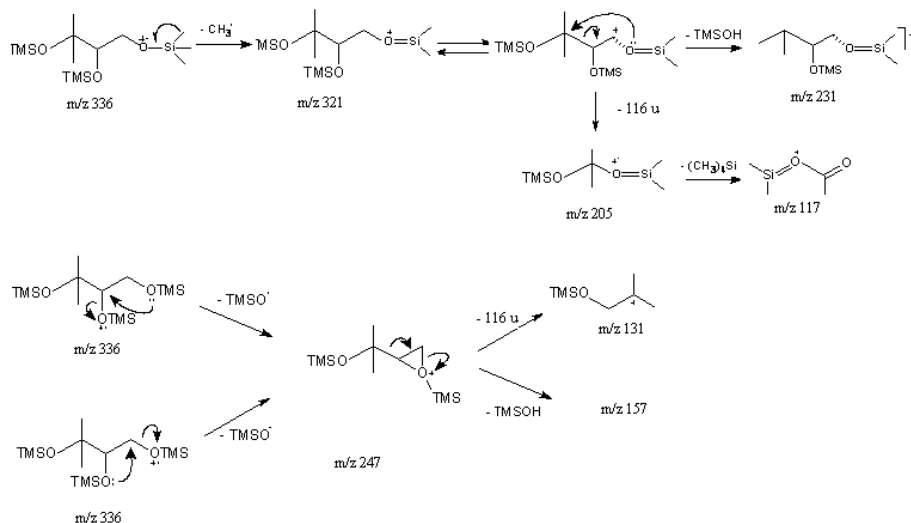
Printer-friendly Version

Interactive Discussion



SOA formation from  
the atmospheric  
oxidation of MBO

M. Jaoui et al.



**Scheme 1.** Proposed fragmentation pathways for silylated compound 20 in EI mode.

Title Page

Abstract

Introduction

Conclusions

References

Tables

Figures

◀

▶

◀

▶

Back

Close

Full Screen / Esc

Printer-friendly Version

Interactive Discussion

